Supporting Information

Synthesis of Highly Uniform and Composition Controlled Gold-Palladium Supported Nanoparticles by Continuous Flow

Stefano Cattaneo[a*], Sultan Althahban[b], Simon J. Freakley[a,c], Meenakshisundaram Sankar[a], Thomas Davies[a], Qian He[a], Nikolaos Dimitratos[a], Christopher J. Kiely[a,b] and Graham. J. Hutchings[a,*]

[a] Cardiff Catalysis Institute, School of Chemistry, Cardiff University, Cardiff, CF10 3AT, United Kingdom.

[b] Department of Materials Science and Engineering, Lehigh University, 5 East Packer Avenue, Bethlehem, Pennsylvania 18015, USA.

[c] Department of Chemistry, University of Bath, Claverton Down, Bath, BA2 7AY, UK.

*CattaneoS@cardiff.ac.uk; Hutch@cardiff.ac.uk

Figure S1: Principle of operation of the I-shape connector geometry, which was found to be optimal in this work.

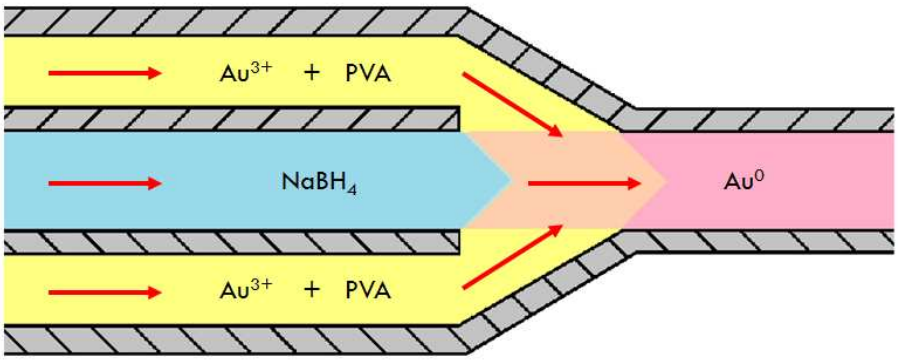

Figure S2: All the UV-vis spectra shown here have been processed by baseline subtraction from the original spectra (seen in the inset). The apparent absorption after 600 nm is simply a mathematical artefact caused by the subtraction of a straight line (baseline) and has no scientific meaning.

a) UV-vis analysis showing the plasmon resonance feature at different flow rates. The insets show the entire UV-vis spectra and the spectrum of the unreduced metal precursor. The data was recorded using the *in-line* UV-vis flow-cell positioned 50 cm downstream from the T-connection where the Au precursor, PVA and $NaBH_4$ first come into intimate contact.

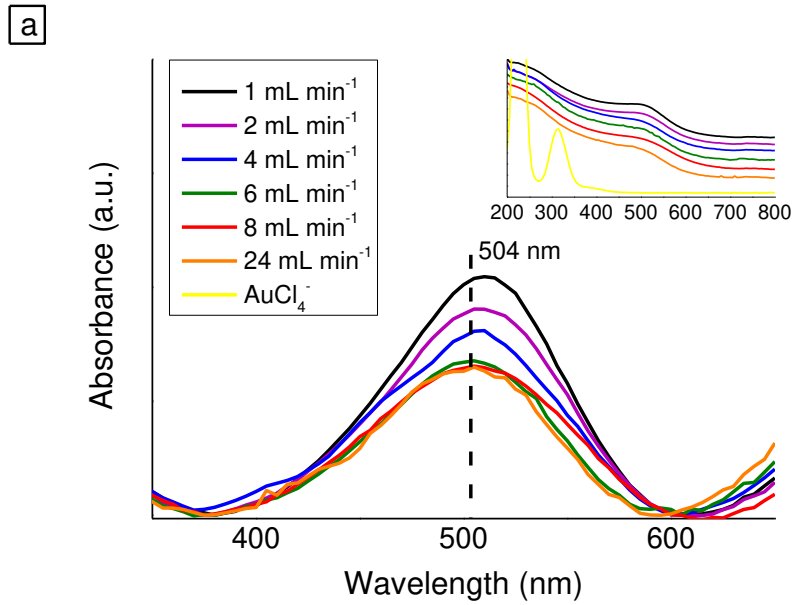

b) UV-vis analysis showing the plasmon resonance for different PVA/Au weight ratios. The insets show the entire UV-vis spectra. The data was recorded using the *in-line* UV-vis flow-cell positioned 50 cm downstream from the T-connection where the Au precursor, PVA and $NaBH_4$ first come into intimate contact.

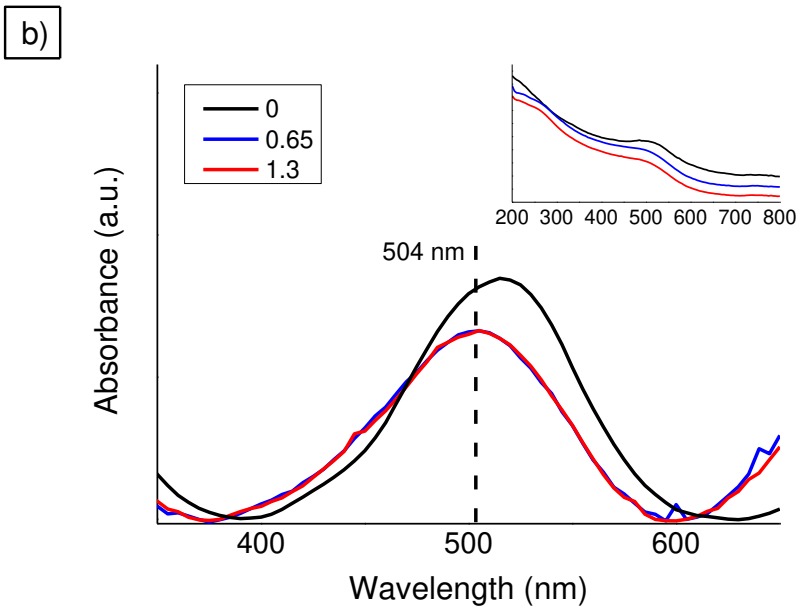

c) UV-vis analysis showing the plasmon resonance for different $NaBH_4$/Au molar ratios. The insets show the entire UV-vis spectra. The data was recorded using the *in-line* UV-vis flow-cell positioned 50 cm downstream from the T-connection where the Au precursor, PVA and $NaBH_4$ first come into intimate contact.

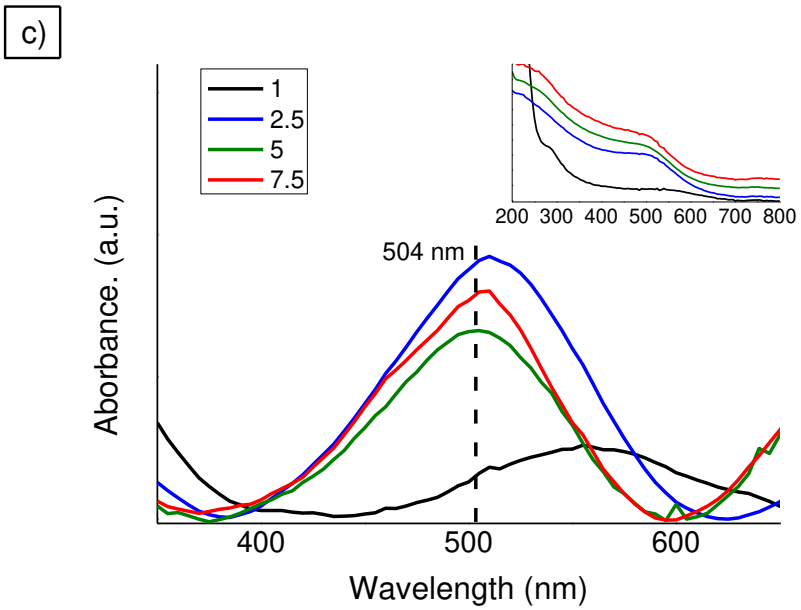

d) UV-vis analysis showing the plasmon resonance with different connector/reactor geometry combinations. The insets show the entire UV-vis spectra. The data was recorded using the *in-line* UV-vis flow-cell positioned 50 cm downstream from the connection where the Au precursor, PVA and $NaBH_4$ first come into intimate contact.

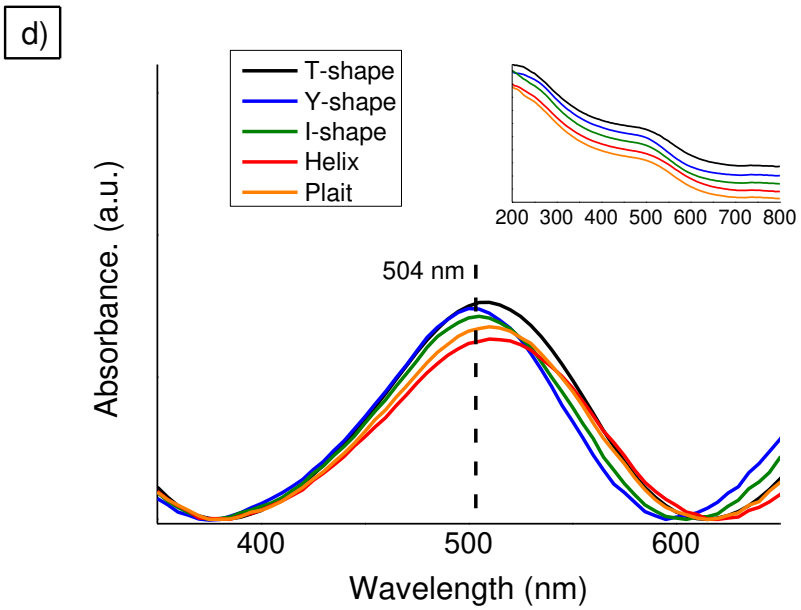

e) UV-vis analysis showing the plasmon resonance with the batch, semi-continuous and continuous synthesis routes. The insets show the entire UV-vis spectra. The data was recorded using the in-line UV-vis flow-cell positioned 50 cm downstream from the T-connection where the Au precursor, PVA and $NaBH_4$ first come into intimate contact.

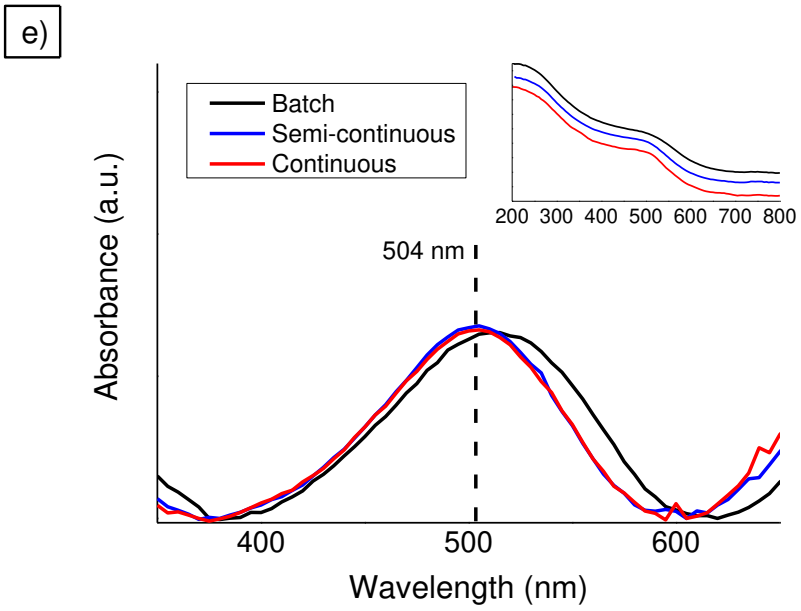

Figure S3: a) Representative DF-STEM image of the Au/TiO_2 *batch* catalyst with b) its corresponding particle size distribution. c) Representative bright field TEM image of the $AuPd/TiO_2$ *batch* catalyst with b) its corresponding particle size distribution.

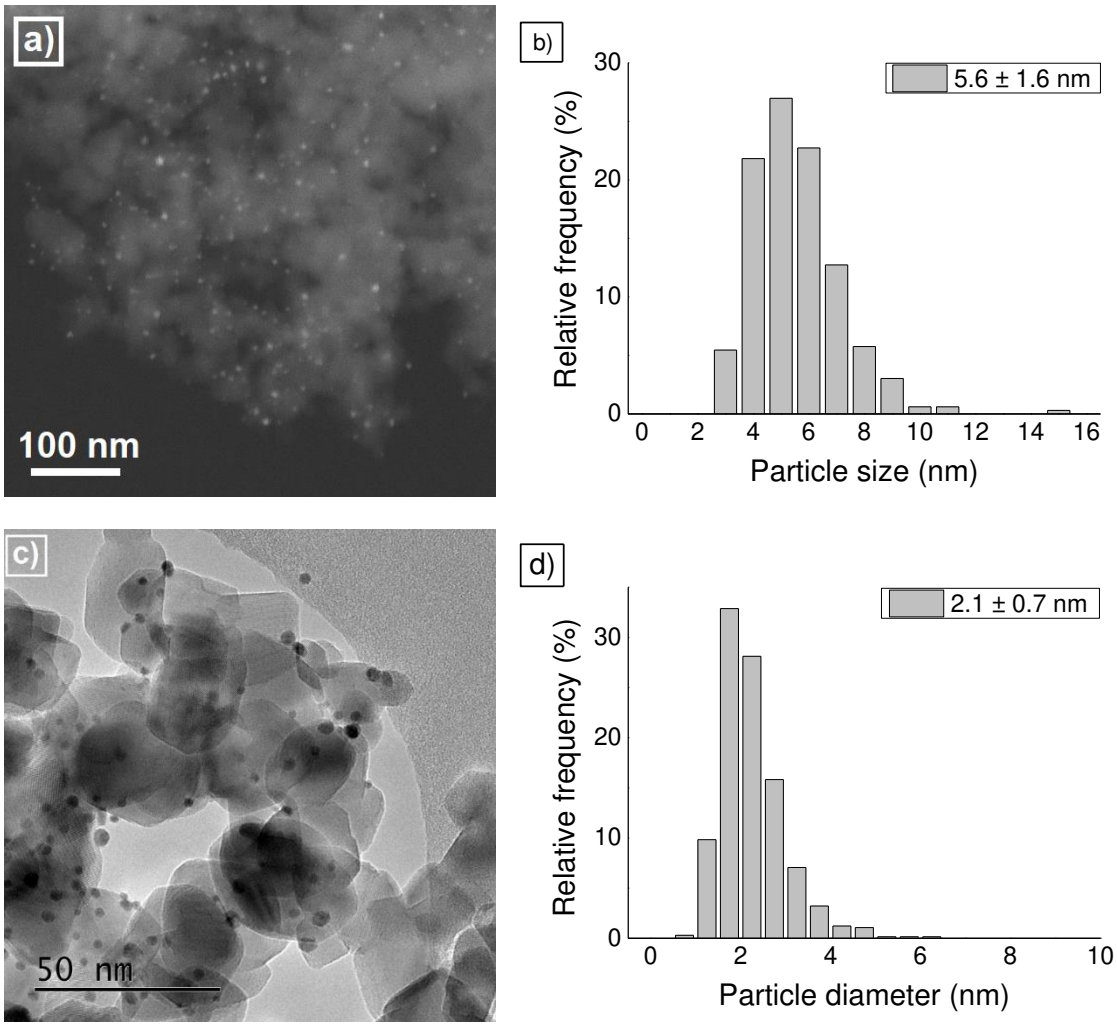

Figure S4: Diffuse reflectance UV-vis analysis of the Au/TiO_2 catalysts prepared via the conventional *batch*, *semi-continuous* and *continuous* production methods.

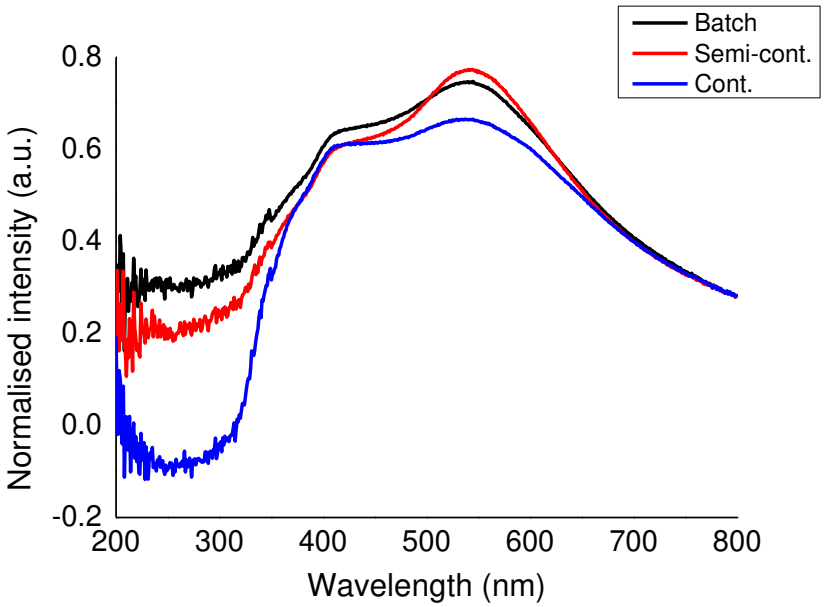

Figure S5: a) Au $4f_{7/2}$ XPS spectra obtained from the Au/TiO_2 and $AuPd/TiO_2$ materials prepared by the *batch*, *semi-continuous* and *continuous* production methods.

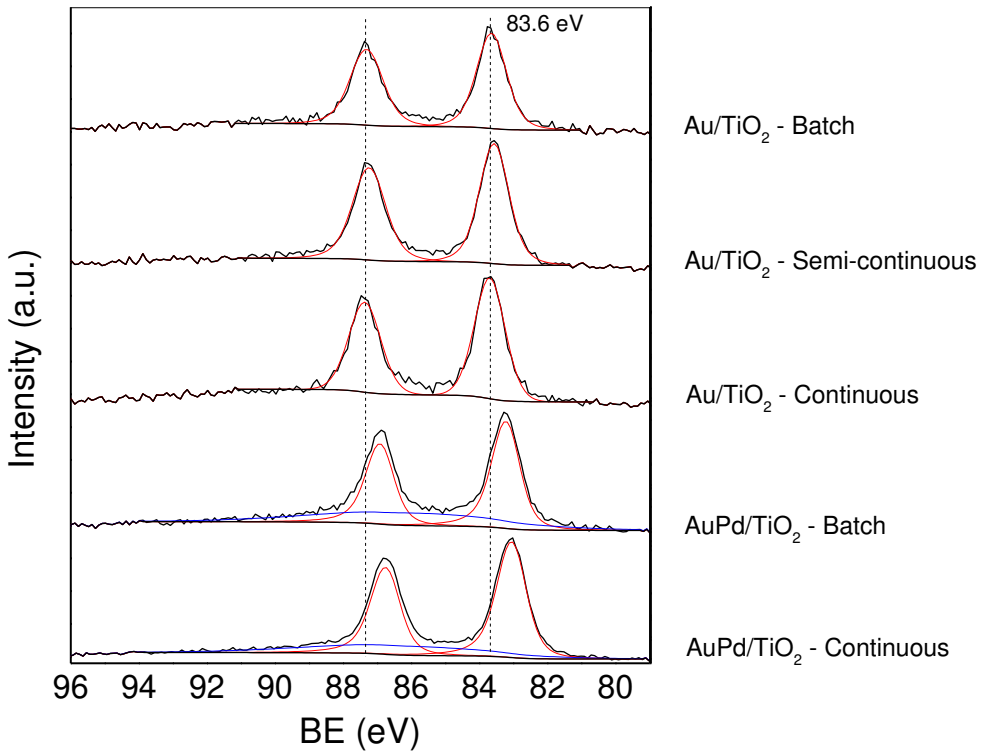

b) Pd $3d_{5/2}$ XPS spectra of $AuPd/TiO_2$ materials prepared by the conventional *batch* and *continuous* production methods.

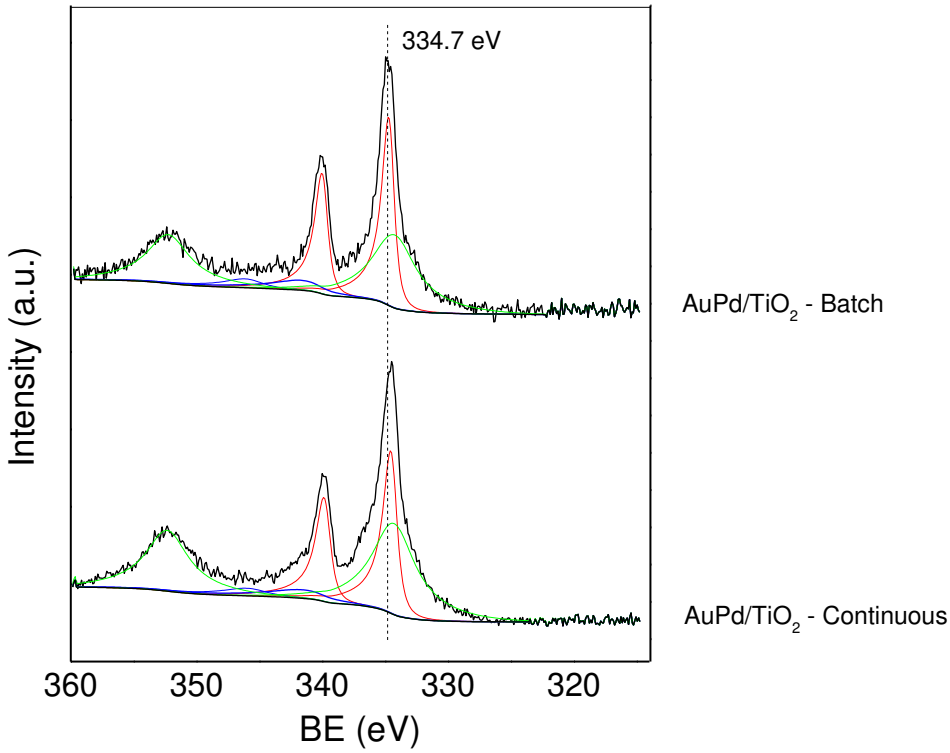

Figure S6: a) Typical time sequence UV-vis spectra following the catalytic reduction of 4-NPH reduction (and more generally of NAR reduction) over Au/TiO_2 made using the *continuous* preparation method with an excess of $NaBH_4$ at room temperature. Molar ratios of Au : NAR : $NaBH_4$ are 1 : 2.5 : 250.

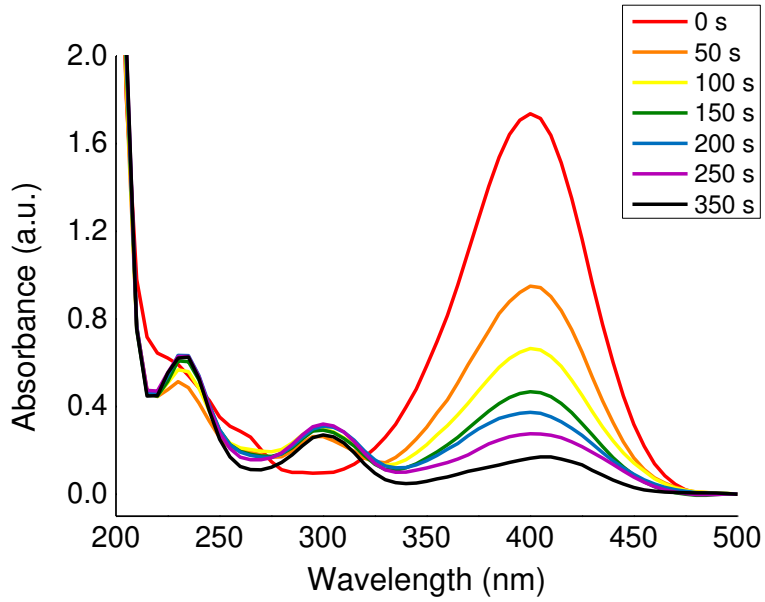

b) Typical plots of C_t/C_0 (black line) and $-\ln(C_t/C_0)$ (red line) versus the reaction time for the reduction of NAR catalysed by Au/TiO_2 made using the *continuous* preparation method with an excess of $NaBH_4$ at room temperature. Molar ratios of Au : NAR : $NaBH_4$ are 1 : 2.5 : 250.

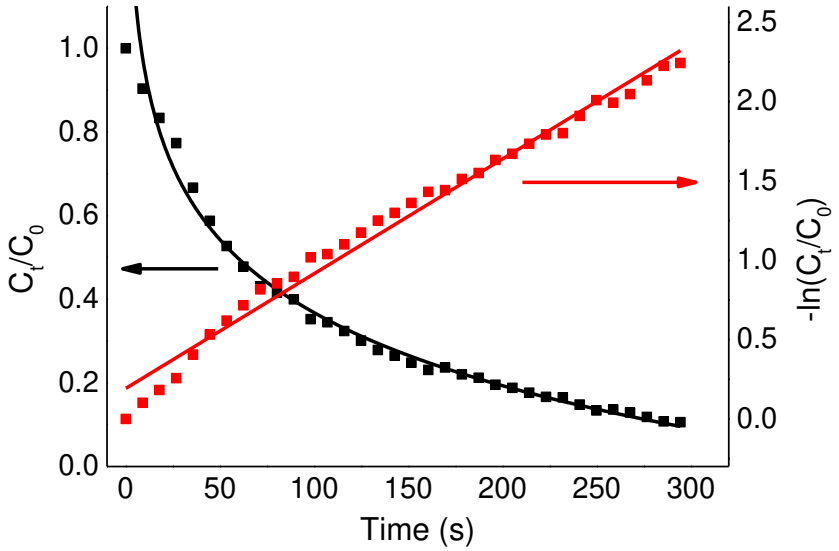

Figure S7: Graphical plot of mean particle size versus flow rate for the continuous production of Au nanoparticles.

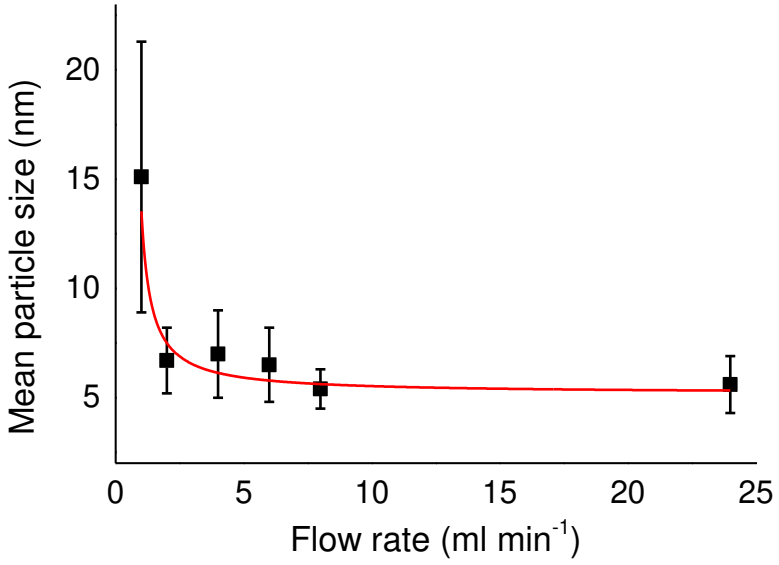

Table S1: Comparison between the *batch* benchmark, *semi-continuous* and *continuous* derived Au/TiO_2 and $AuPd/TiO_2$ catalysts showing mean particle size, metal loading, and Au $4f_{7/2}$ and Pd $3d_{5/2}$ binding energies.

Catalyst	Mean NP size [nm]		Metal loading	Binding energy [eV]	
	DLS	DF-STEM	[wt%]	Au $4f_{7/2}$	Pd $3d_{5/2}$
Au/TiO_2 - batch	5.6 ± 1.7	5.6 ± 1.6	0.94	83.6	-
Au/TiO_2-semi-continuous	6.0 ± 1.7	5.4 ± 0.9	0.92	83.7	-
Au/TiO_2 - continuous	5.4 ± 1.6	4.5 ± 1.3	0.96	83.6	-
$AuPd/TiO_2$ - batch	7.7 ± 2.1	2.1 ± 0.7	0.95	83.2	334.7
$AuPd/TiO_2$ - continuous	7.6 ± 2.3	2.0 ± 0.7	0.94	83.0	334.6

References

1 T. Aditya, A. Pal and T. Pal, *Chem. Commun.*, **2015**, *51*, 9410–9431.